

Bioinspired desaturation of alcohols enabled by photoredox proton-coupled electron transfer and cobalt dual catalysis

Long Huang ^{1✉}, Tengfei Ji¹, Chen Zhu², Huifeng Yue², Nursaya Zhumabay ² & Magnus Rueping ^{2✉}

In the biosynthesis sterols an enzyme-catalyzed demethylation is achieved via a stepwise oxidative transformation of alcohols to olefins. The overall demethylation proceeds through two sequential monooxygenation reactions and a subsequent dehydroformylative saturation. To mimic the desaturation processes observed in nature, we have successfully integrated photoredox proton-coupled electron transfer (PCET) and cobaloxime chemistry for the acceptorless dehydrogenation of alcohols. The state-of-the-art remote and precise desaturation of ketones proceeds efficiently through the activation of cyclic alcohols using bond-dissociation free energy (BDFE) as thermodynamic driving force. The resulting transient alkoxyl radical allows C-C bond scission to generate the carbon-centered radical remote to the carbonyl moiety. This key intermediate is subsequently combined with cobaloxime photochemistry to furnish the alkene. Moreover, the mild protocol can be extended to desaturation of linear alcohols as well as aromatic hydrocarbons. Application to bioactive molecules and natural product derivatives is also presented.

¹Institute of Organic Chemistry, RWTH Aachen University, Landoltweg 1, 52074 Aachen, Germany. ²Kaust Catalysis Center (KCC), King Abdullah University of Science and Technology (KAUST), Thuwal 23955-6900, Saudi Arabia. ✉email: long.huang@rwth-aachen.de; magnus.rueping@kaust.edu.sa

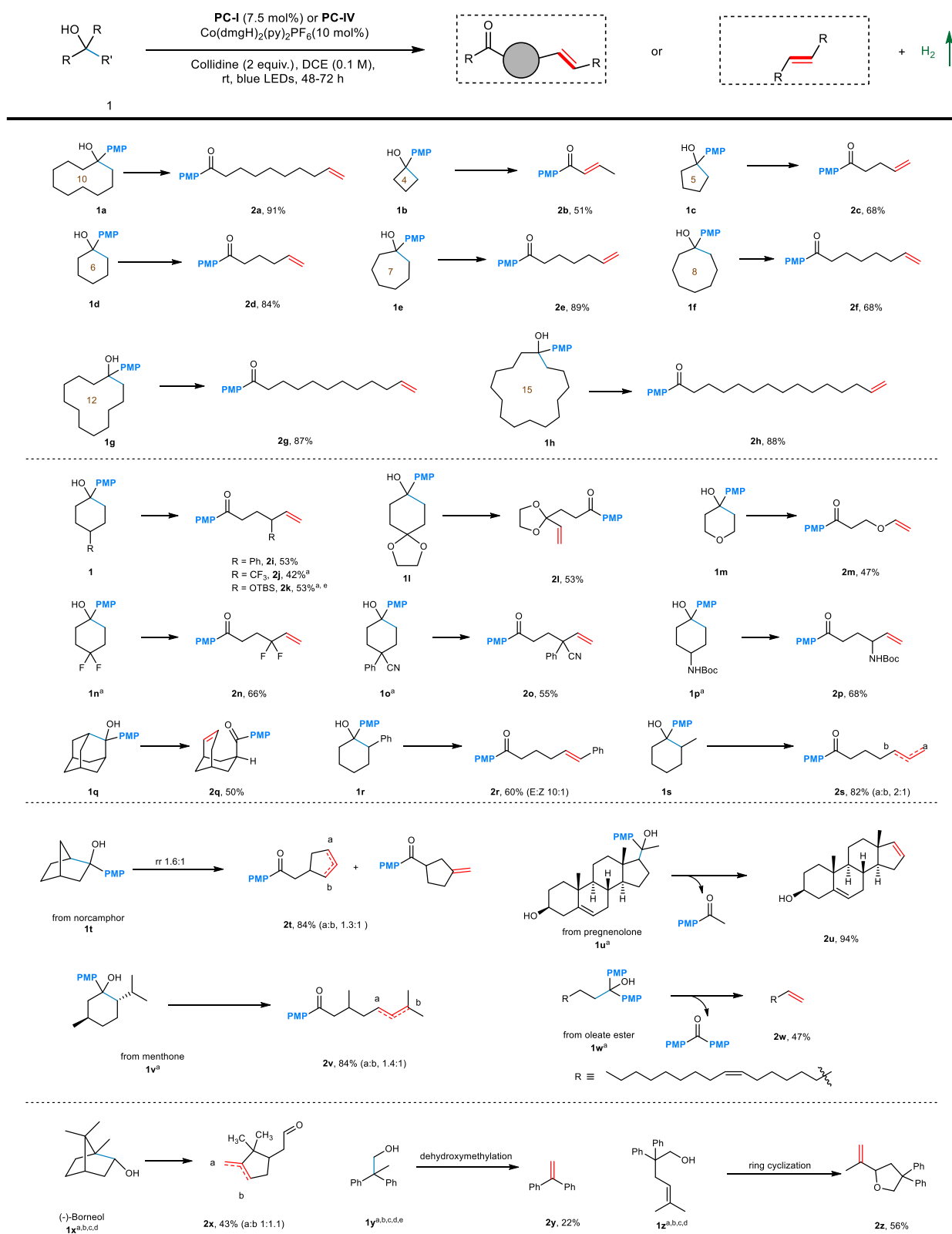


Fig. 3 Scope of cyclic and linear alcohols. General reaction conditions: **1** (1 equiv.), 2,4,6-collidine (2 equiv.), **PC-I** (7.5 mol%), Co(dmgH)₂(py)₂PF₆ (10 mol%), DCE (0.1 M), rt, blue LEDs, 48–72 h. **a** 1 or 3 mol% [Ir(dF(CF₃)ppy)₂(5,5'-d(CF₃)bpy)](PF₆) **PC-IV** was used. **b** NBu₄OP(O)(OPh)₂ as base. **c** Toluene or PhCF₃ as solvent. **d** 5 mol% Co catalyst was used in **2u** to **2z**. **e** ¹H NMR yield with internal standard.

secondary alcohols, via the photoredox PCET and cobalt synergistic catalysis and the extension to the desaturation to aromatic hydrocarbons, as well as silyl enol ethers.

Results

Rational design. Our mechanistic proposal is shown in Fig. 2. Upon visible light irradiation, a single electron transfer from the cyclohexanol derivative ($E_{P/2} = 1.57$ V vs. SCE)¹⁶ to the highly oxidizing singlet excited state $^*\text{Mes-Acr-Me}^+$ ($E_{1/2}^{\text{red}} = +2.06$ V vs. SCE)⁶ would generate the corresponding arene radical cation along with the reduced form of the photocatalyst **Mes-Acr-Me**. Subsequent multiple site PCET reaction between the hydroxyl group and the radical cation in the presence of base would give the key alkoxy radical species, which readily cleaves into a carbonyl moiety and a distal carbon-centered radical through β scission of the neighboring C-C bond. The C-centered radical would subsequently be intercepted by the Co^{II} species (**I**) to yield an alkyl- Co^{III} intermediate (**II**), which can undergo C-cobalt bond homolysis upon light irradiation. Next, a β -hydrogen abstraction by Co^{II} at this stage would deliver the desired olefin and a cobalt^{III} hydride species (**III**). Hydrogen gas evolves through the interaction between (**III**) and a proton generated in the PCET step. The cobalt and photoredox catalytic cycles then simultaneously complete via a single electron transfer event between Co^{III} intermediate (**IV**) ($E_{1/2}^{\text{red}} = -0.68$ V vs. SCE) and reduced form of photocatalyst **C**^{56,57}.

Optimization of the reaction conditions. The reaction conditions optimization of the synergistic combination of photoredox and cobalt catalysis is briefly summarized in Table 1. The initial evaluation focused on readily available substrate **1a** to mimic the enzymatic process, namely Δ^9 desaturation of stearyl-CoA (Fig. 1c). Optimized reaction conditions were readily established,

using 7.5 mol% **PC-I** Mes-Acr-Me⁺, 10 mol% $\text{Co}(\text{dmgH})_2(\text{py})_2\text{PF}_6$ and 2 equiv. 2,4,6-collidine in a 0.1 M solution of 1,2-dichloroethane (DCE) at room temperature with blue light-emitting diodes (LEDs) irradiation. Under these conditions, the desired product was formed in 93% NMR yield and very good selectivity (22:1) (Table 1, entry 1). Use of less oxidizing photosensitizers such as $[\text{Ru}(\text{bpy})_3](\text{PF}_6)_2$ (**PC-II**, $E_{1/2}[\text{Ru}^{\text{III}}/\text{Ru}^{\text{II}}] = +0.77$ V vs. SCE in CH_3CN)⁵⁸ and $[\text{Ir}(\text{dF}(\text{CF}_3)\text{ppy})_2(\text{bpy})]\text{PF}_6$ (**PC-III**, $E_{1/2}[\text{Ir}^{\text{III}}/\text{Ir}^{\text{II}}] = +1.21$ V vs. SCE in CH_3CN)⁵⁹ resulted in no product or trace amounts of product, while the strong oxidizing $[\text{Ir}(\text{dF}(\text{CF}_3)\text{ppy})_2(5,5'(\text{CF}_3)\text{bpy})]\text{PF}_6$ (**PC-IV**, $E_{1/2}[\text{Ir}^{\text{III}}/\text{Ir}^{\text{II}}] = +1.68$ V vs. SCE in CH_3CN) gave **2a** in 71% yield (entries 2 to 4). A screening of different organic and inorganic bases revealed that collidine was the best choice (entries 5 and 6). The use of $\text{Co}(\text{dmgH})(\text{dmgH}_2)\text{Cl}_2$ and $\text{Co}(\text{dmgH})_2\text{PyCl}$ as cobaloxime sources leads to a decrease of yields and selectivities (entries 7 and 8). When the reaction was conducted in HFIP or MeCN, the amount of product could be negligible. The reaction efficiency diminished dramatically when toluene was employed, while a comparable result was observed using DCM (entries 9–12). The inverse relationship between solvent polarity and yield can be taken as support for the intermediacy of hydrogen bonding, because the polar interaction is generally disfavored in polar solvent. It is not surprising to observe that control experiments performed without photocatalyst, Co catalyst, base or light each failed to give any desired product (Table 1, entry 13).

Substrate scope. As illustrated in Fig. 3, we found the desaturation protocol was tolerant to a wide range of alcohols and gave the corresponding olefinic products in moderate to very good yields. To begin with, it was found that cyclic tertiary alcohols with different ring sizes (**1a–1h**) all reacted smoothly to selectively generate remote desaturated ketones regardless of their ring strains (**2a–h**, 51–91% yields). Notably, due to the base mediated isomerization,

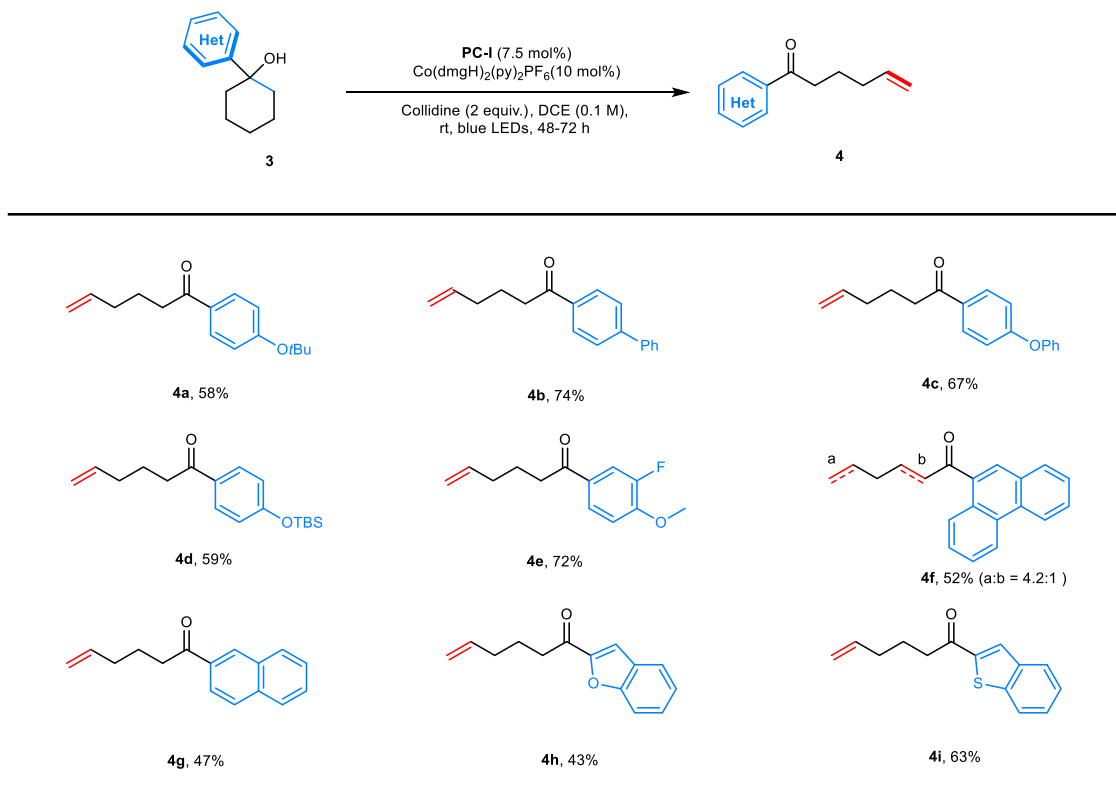


Fig. 4 Scope of arene substituents. Reaction conditions: **3** (0.2 mmol, 1 equiv.), 2,4,6-collidine (0.4 mmol, 2 equiv.), **PC-I** (7.5 mol%), $\text{Co}(\text{dmgH})_2(\text{py})_2\text{PF}_6$ (10 mol%), DCE (2.0 mL, 0.1 M), rt, blue LEDs, 48–72 h.

the α - β -sites desaturation product was obtained exclusively with prolonged reaction time in the reaction of cyclobutanol **1b**. Symmetrical substituted cyclohexanols (**1i** to **1p**) behaved well to give products **2i** to **2p** in moderate yields (42–68%). Functional groups including trifluoromethyl, silyl ether, geminal difluoride, nitrile and amide could be well tolerated. The ring-opening of unsymmetrical cyclohexanols **1r** and **1s** took place regioselectively and, the remarkable selectivity can be explained by C–C bond cleavage favors the formation of more stabilized carbon-centered radical (**2r** and **2s**, 60% and 82% yields).

For the norcamphor-derived bridged bicyclic substrate **1t**, mixture of isomers was observed as a result of poor selectivity in the ring-opening. In contrast, a menthone derivative displays excellent regioselectivity in the ring-opening step (**1v**, 84%).

Moreover, we successfully extended the scope to linear tertiary alcohols derived from pregnenolone and oleate ester, affording the corresponding olefins **2u** and **2w** in moderate to excellent yields. In addition to tertiary alcohols, naturally occurring secondary alcohol **1x** proved to be competent substrate for the PCET enabled regioselective ring-opening/desaturation sequence. Remarkably, the dehydroxymethylative desaturation of 2,2-diphenylpropan-1-ol could take place, affording the diphenylethylene in 22% yield. Next, we found that the cascade ring cyclization/desaturation was feasible, a moderate yield of cyclized product was obtained (**2z**, 56%).

With the above success, we next examined the generality of the photoredox-cobalt desaturation with respect to the arene substituent on the cyclic ring. As shown in Fig. 4, a variety of

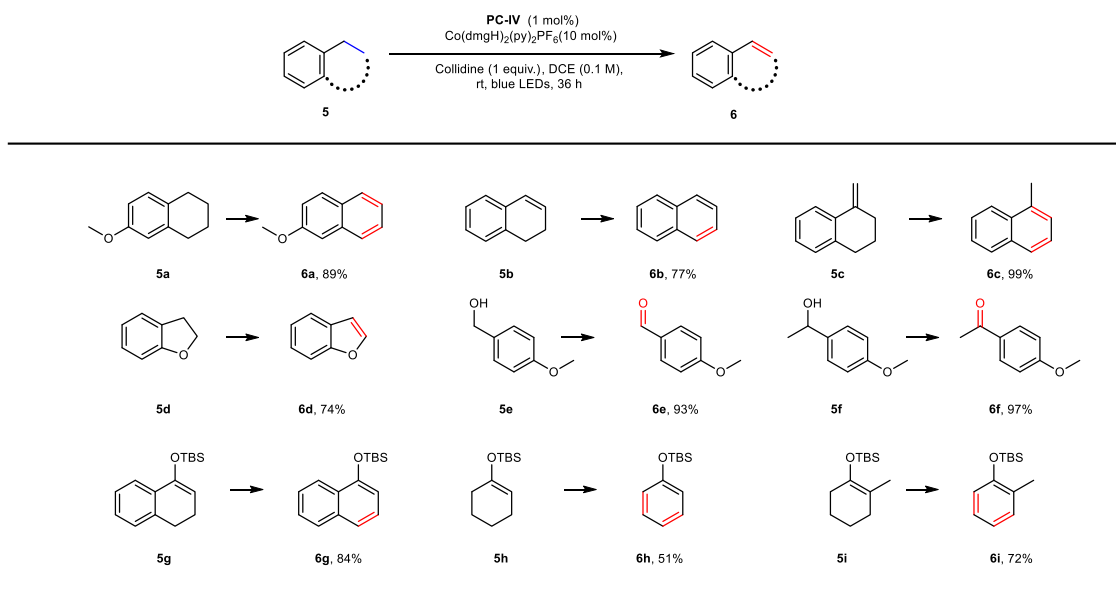


Fig. 5 Scope of aromatic hydrocarbons and silyl enol ether. Reaction conditions: **5** (0.2 mmol, 1 equiv.), 2,4,6-collidine (0.2 mmol, 1 equiv.), [Ir(dF(CF₃)ppy)₂(5,5'-d(CF₃)bpy)](PF₆)₂ **PC-IV** (1 mol%), Co(dmgH)₂(py)₂PF₆ (10 mol%), DCE (1.0 mL, 0.2 M), rt, blue LEDs, 36 h.

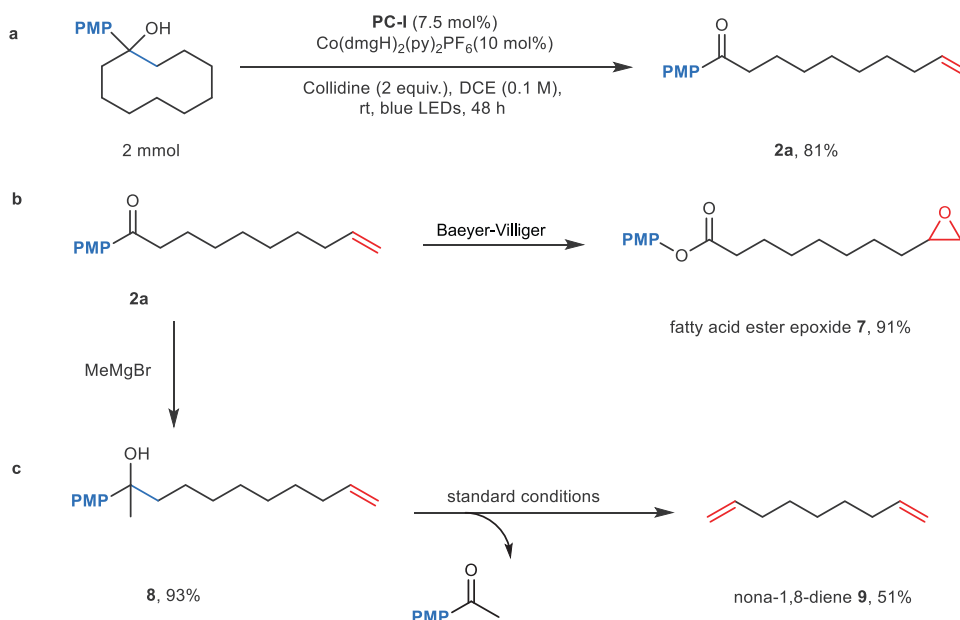


Fig. 6 Scale up and synthetic utility. **a** Reaction on large scale, under standard conditions: tertiary alcohol (1 equiv.), 2,4,6-collidine (2 equiv.), **PC-I** (7.5 mol%), Co(dmgH)₂(py)₂PF₆ (10 mol%), DCE (0.1 M), rt, blue LEDs, 48 h. **b** Baeyer-villiger oxidation. **c** sequential desaturation to synthesize diene.

arene-substituted cyclohexanols performed well. Monosubstituted aromatics such as *tert*-butyl-, phenyl-, and *tert*-butyldimethylsilyl (TBS)-protected phenols as well as biphenyl are suitable candidates (**4a–4d**, 58–74% yields). Disubstituted anisole derivative was also suitable substrate for this transformation (**4e**, 72% yield). Both naphthalene- and phenanthrene-substituted cyclohexanols smoothly underwent ring-opening/desaturation under these conditions (**4f** and **4g**, 52% and 47% yields). Interestingly, minor amount of α -/ β -sites desaturation product was obtained in the case of **4f**, this can be accounted for by Co^{III}-hydride mediated chain walking process⁵¹. Following the success, privileged heteroaromatics including benzofuran and thienobenzofuran could also be used (**4h** and **4i**, 43% and 63% yields).

To further highlight the robustness of this protocol, tetrahydronaphthalene **5a** was subjected to the reaction conditions (Fig. 5). The desaturation takes place selectively to release 2 molar equiv. hydrogen gas and no dihydronaphthalene product was observed, indicating the second desaturation should be easier than the initial

one. Therefore, two styrene derivatives were examined next, to give products such as **6b** and **6c** in good to excellent yields. Heterocycle such as **6d** can also be prepared in good yield (74%). Moreover, when benzylic alcohols were employed in the PCET enabled acceptorless desaturation, the corresponding aldehyde and ketone products were obtained in excellent yields (**6e** and **6f**). Importantly, this protocol was able to transform silyl enol ethers into silyloxyarenes in moderate to good yields⁶⁰. For example, desaturation of **5g** leads to the formation of *tert*-butyl(dimethyl)silyl (TBS) ether of α -naphthol with excellent efficiency (**6g**, 84% yield). Silyl enol ethers derived from cyclohexanones were also amenable to the current protocol via the removal of two molecules of hydrogen gas, with no detection of α , β -desaturated ketone product (**6h** and **6i**, 51% and 72% yields, respectively). This intriguing selectivity stands in stark contrast to previous dehydrogenation reactions that exclusively affording cyclohexenones^{61,62}.

Next, we carried out the synthesis of remote unsaturated ketone **2a** on a preparative scale (2 mmol) under our optimal

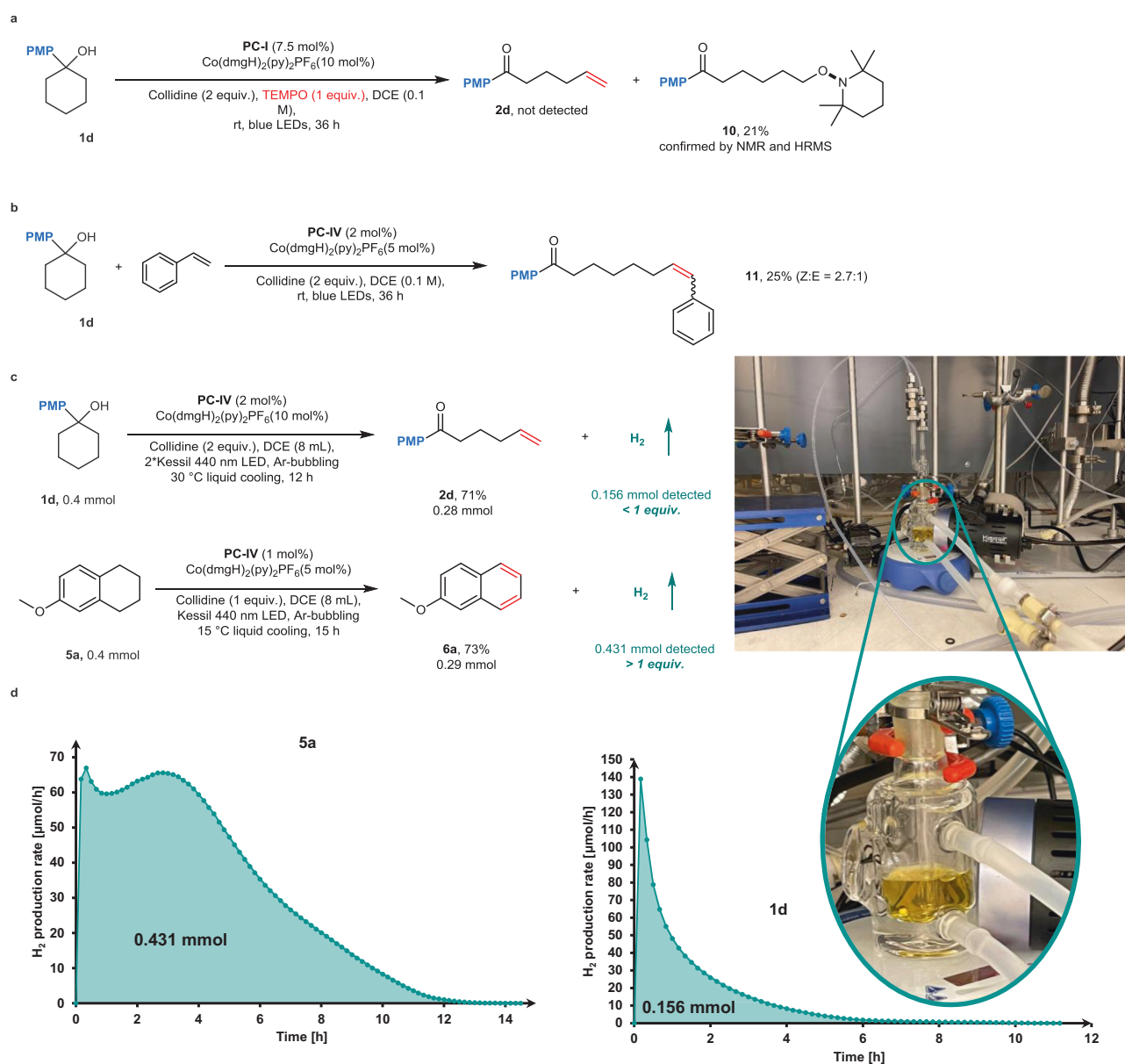


Fig. 7 Preliminary experiments on the reaction mechanism. **a** Radical-trapping experiment with free-radical scavenger. **b** Heck-Type coupling with styrene. **c** Reaction conditions and results for H₂ production of substrates **1d** and **5a**. **d** H₂ production rate monitoring and quantification for substrates **1d** and **5a**.

conditions, providing the expected olefinic product **1a** in 81% yield (Fig. 6a). To showcase the synthetic utility of the product provided by this methodology, **2a** was converted efficiently to a fatty acid ester epoxide during a Baeyer-Villiger oxidation (Fig. 6b). Following a Grignard reaction of **2a**, the linear product **8** was subjected further to the reaction conditions, an interesting diene **9** was isolated in 51% yield (Fig. 6c).

Apart from the control experiments shown in Table 1, we conducted some preliminary mechanistic experiments to gain some insight of the metallaphotoredox desaturation protocol. When the reaction mixture was subjected to a radical scavenger 2,2,6,6-Tetramethyl-1-piperidinyloxy (TEMPO, 1 equiv.) under the standard conditions, no product was detected. A remote TEMPO-trapped ketone **10** was instead formed, implying that a radical process is involved in the catalytic cycle (Fig. 7a). The generation of carbon-centered radical remote to the carbonyl group was further supported by the Heck-Type coupling with styrene, affording **11** (Fig. 7b). To gain more insight into the reaction, the formation of molecular hydrogen was quantitatively analyzed by gas chromatography. Importantly, we observed that more than 1 equiv. hydrogen gas was produced with substrate **5a**, in contrast the generation of H₂ is less than 1 equiv. in the case of **1d**. The kinetic profile of H₂ evolution of substrate **1d** shows a fast gas production rate in the first hours, however, it becomes very sluggish after 6 h (Fig. 7c, d). This result is consistent with our observation that the desaturation of alcohols generally required long reaction time, we assume that the increasing amount of free base has a marked effect on the hydrogen production⁶³.

Discussion

In conclusion, we have developed a bioinspired acceptorless desaturation of tertiary as well as secondary alcohols *via* the photoredox PCET and cobalt synergistic catalysis. The manifold provides a concise access to remotely dehydrogenated ketones that are difficult to synthesize with current methods, through ring-opening/desaturation of cyclic alcohols. We also demonstrated the strategy could be applied to linear alcohol, aromatic hydrocarbons as well as silyl enol ethers. Importantly, a variety of bioactive molecules and natural product derivatives were all well tolerated under such mild conditions. In consideration with numerous findings about the essential role of PCET in biological redox processes, this contribution expands the less-developed applications of PCET in organic synthesis.

Methods

General procedure for bioinspired dehydrogenation of alcohols. To a 15 mL vial equipped with a stir bar was added Co(dmgH)₂(py)₂PF₆ (12 mg, 0.02 mmol, 10 mol%), and photocatalyst (9-mesityl-10-methylacridinium perchlorate 7.5 mol% or [Ir(dF(CF₃)ppy)₂(5,5'-d(CF₃)bpy)](PF₆) 1 mol%), collidine (1 or 2 equiv.) and tertiary alcohol (0.2 mmol, 1 equiv.). The vial was sealed, evacuated and backfilled with Argon three times, then 2 mL of DCE was added. After degassing with Freeze-Pump-Thaw methods for three cycles, it was stirred and irradiated with the corresponding blue LEDs photoreactor. Upon completion, the reaction mixture was concentrated *in vacuo* and purified with column chromatography to afford the desired product.

Data availability

The authors declare that all data generated in this study are available within the article and the Supplementary Information.

Received: 20 July 2021; Accepted: 20 January 2022;

Published online: 10 February 2022

References

- Shyadehi, A. Z. et al. The mechanism of the acyl-carbon bond cleavage reaction catalyzed by recombinant sterol 14 α -demethylase of *Candida albicans* (other names are: lanosterol 14 α -demethylase, P-45014DM, and CYP51). *J. Biol. Chem.* **271**, 12445–12450 (1996).

- Lepesheva, G. I. & Waterman, M. R. Sterol 14 α -demethylase cytochrome P450 (CYP51), a P450 in all biological kingdoms. *Biochim. Biophys. Acta* **1770**, 467–477 (2007).
- Lepesheva, G. I. & Waterman, M. R. Structural basis for conservation in the CYP51 family. *Biochim. Biophys. Acta* **1814**, 88–93 (2011).
- Yoshida, Y. in *Cytochrome P450* (eds Schenkman, J. B. & Greim, H.) 627–639 (Springer Berlin Heidelberg, 1993).
- Blanksby, S. J. & Ellison, G. B. Bond dissociation energies of organic molecules. *Acc. Chem. Res.* **36**, 255–263 (2003).
- Romero, N. A. & Nicewicz, D. A. Organic photoredox catalysis. *Chem. Rev.* **116**, 10075–10166 (2016).
- Shaw, M. H., Twilton, J. & MacMillan, D. W. C. Photoredox catalysis in organic chemistry. *J. Org. Chem.* **81**, 6898–6926 (2016).
- Xie, J., Jin, H. & Hashmi, A. S. K. The recent achievements of redox-neutral radical C–C cross-coupling enabled by visible-light. *Chem. Soc. Rev.* **46**, 5193–5203 (2017).
- Chen, Y., Lu, L.-Q., Yu, D.-G., Zhu, C.-J. & Xiao, W.-J. Visible light-driven organic photochemical synthesis in China. *Sci. China Chem.* **62**, 24–57 (2019).
- Kancherla, R., Muralirajan, K., Sagadevan, A. & Rueping, M. Visible Light-induced excited-state transition-metal catalysis. *Trends Chem.* **1**, 510–523 (2019).
- Jia, K., Zhang, F., Huang, H. & Chen, Y. Visible-light-induced alkoxy radical generation enables selective C(sp³)–C(sp³) bond cleavage and functionalizations. *J. Am. Chem. Soc.* **138**, 1514–1517 (2016).
- Hu, A. et al. Cerium-catalyzed formal cycloaddition of cycloalkanols with alkenes through dual photoexcitation. *J. Am. Chem. Soc.* **140**, 13580–13585 (2018).
- Hu, A., Guo, J.-J., Pan, H. & Zuo, Z. Selective functionalization of methane, ethane, and higher alkanes by cerium photocatalysis. *Science* **361**, 668–672 (2018).
- Schwarz, J. & König, B. Visible-light mediated C–C bond cleavage of 1,2-diols to carbonyls by cerium-photocatalysis. *Chem. Commun.* **55**, 486–488 (2019).
- Zhang, K., Chang, L., An, Q., Wang, X. & Zuo, Z. Dehydroxymethylation of alcohols enabled by cerium photocatalysis. *J. Am. Chem. Soc.* **141**, 10556–10564 (2019).
- Huang, L., Ji, T. & Rueping, M. Remote nickel-catalyzed cross-coupling arylation via proton-coupled electron transfer-enabled C–C bond cleavage. *J. Am. Chem. Soc.* **142**, 3532–3539 (2020).
- Guo, J.-J. et al. Photocatalytic C–C bond cleavage and amination of cycloalkanols by cerium(III) chloride complex. *Angew. Chem. Int. Ed.* **55**, 15319–15322 (2016).
- Hu, A. et al. δ -selective functionalization of alkanols enabled by visible-light-induced ligand-to-metal charge transfer. *J. Am. Chem. Soc.* **140**, 1612–1616 (2018).
- Chen, Y., Du, J. & Zuo, Z. Selective C–C bond scission of ketones via visible-light-mediated cerium. *Catal. Chem.* **6**, 266–279 (2020).
- Ji, T., Chen, X.-Y., Huang, L. & Rueping, M. Remote trifluoromethylthiolation enabled by organophotocatalytic C–C bond cleavage. *Org. Lett.* **22**, 2579–2583 (2020).
- Wang, D., Mao, J. & Zhu, C. Visible light-promoted ring-opening functionalization of unstrained cycloalkanols via inert C–C bond scission. *Chem. Sci.* **9**, 5805–5809 (2018).
- Zhao, R. et al. Visible-light-enhanced ring opening of cycloalkanols enabled by brønsted base-tethered acyloxy radical induced hydrogen atom transfer-electron transfer. *Org. Lett.* **20**, 1228–1231 (2018).
- Wu, X., Cruz, F. A., Lu, A. & Dong, V. M. Tandem catalysis: transforming alcohols to alkenes by oxidative dehydroxymethylation. *J. Am. Chem. Soc.* **140**, 10126–10130 (2018).
- Conia, J. M. & Le Perche, P. The thermal cyclisation of unsaturated carbonyl compounds. *Synthesis* **1975**, 1–19 (1975).
- Houk, K. N. The photochemistry and spectroscopy of β,γ -unsaturated carbonyl compounds. *Chem. Rev.* **76**, 1–74 (1976).
- Shiraki, T. et al. α,β -unsaturated ketone is a core moiety of natural ligands for covalent binding to peroxisome proliferator-activated receptor γ . *J. Biol. Chem.* **280**, 14145–14153 (2005).
- LoPachin, R. M., Barber, D. S. & Gavin, T. Molecular mechanisms of the conjugated α,β -unsaturated carbonyl derivatives: relevance to neurotoxicity and neurodegenerative diseases. *Toxicol. Sci.* **104**, 235–249 (2007).
- Muzart, J. One-pot syntheses of α,β -unsaturated carbonyl compounds through palladium-mediated dehydrogenation of ketones, aldehydes, esters, lactones and amides. *Eur. J. Org. Chem.* **2010**, 3779–3790 (2010).
- Zhang, S., Neumann, H. & Beller, M. Synthesis of α,β -unsaturated carbonyl compounds by carbonylation reactions. *Chem. Soc. Rev.* **49**, 3187–3210 (2020).
- Buist, P. H. Fatty acid desaturases: selecting the dehydrogenation channel. *Nat. Prod. Rep.* **21**, 249–262 (2004).
- Voica, A.-F., Mendoza, A., Gutekunst, W. R., Fraga, J. O. & Baran, P. S. Guided desaturation of unactivated aliphatics. *Nat. Chem.* **4**, 629–635 (2012).

32. Parasram, M., Chuentragool, P., Wang, Y., Shi, Y. & Gevorgyan, V. General, auxiliary-enabled photoinduced Pd-catalyzed remote desaturation of aliphatic alcohols. *J. Am. Chem. Soc.* **139**, 14857–14860 (2017).
33. Chuentragool, P. et al. Aliphatic radical relay heck reaction at unactivated C(sp³)-H sites of alcohols. *Angew. Chem. Int. Ed.* **58**, 1794–1798 (2019).
34. Yayla, H. G., Wang, H., Tarantino, K. T., Orbe, H. S. & Knowles, R. R. Catalytic ring-opening of cyclic alcohols enabled by PCET activation of strong O–H bonds. *J. Am. Chem. Soc.* **138**, 10794–10797 (2016).
35. Ota, E., Wang, H., Frye, N. L. & Knowles, R. R. A redox strategy for light-driven, out-of-equilibrium isomerizations and application to catalytic C–C bond cleavage reactions. *J. Am. Chem. Soc.* **141**, 1457–1462 (2019).
36. Turlik, A., Chen, Y. & Newhouse, T. R. Dehydrogenation adjacent to carbonyls using palladium–allyl intermediates. *Synlett* **27**, 331–336 (2016).
37. Kato, S. et al. Hybrid catalysis enabling room-temperature hydrogen gas release from n-heterocycles and tetrahydronaphthalenes. *J. Am. Chem. Soc.* **139**, 2204–2207 (2017).
38. Chen, M. & Dong, G. Copper-catalyzed desaturation of lactones, lactams, and ketones under pH-neutral conditions. *J. Am. Chem. Soc.* **141**, 14889–14897 (2019).
39. Fuse, H., Mitsunuma, H. & Kanai, M. Catalytic acceptorless dehydrogenation of aliphatic alcohols. *J. Am. Chem. Soc.* **142**, 4493–4499 (2020).
40. Tsukamoto, T. & Dong, G. Catalytic dehydrogenative cyclization of o-teraryls under pH-neutral and oxidant-free conditions. *Angew. Chem. Int. Ed.* **59**, 15249–15253 (2020).
41. U. Dighe, S., Juliá, F., Luridiana, A., Douglas, J. J. & Leonori, D. A photochemical dehydrogenative strategy for aniline synthesis. *Nature* **584**, 75–81 (2020).
42. Weiss, M. E., Kreis, L. M., Lauber, A. & Carreira, E. M. Cobalt-catalyzed coupling of alkyl iodides with alkenes: deprotonation of hydridocobalt enables turnover. *Angew. Chem. Int. Ed.* **50**, 11125–11128 (2011).
43. West, J. G., Huang, D. & Sorensen, E. J. Acceptorless dehydrogenation of small molecules through cooperative base metal catalysis. *Nat. Commun.* **6**, 10093 (2015).
44. Thullen, S. M. & Rovis, T. A mild hydroaminoalkylation of conjugated dienes using a unified cobalt and photoredox catalytic system. *J. Am. Chem. Soc.* **139**, 15504–15508 (2017).
45. Abrams, D. J., West, J. G. & Sorensen, E. J. Toward a mild dehydroformylation using base-metal catalysis. *Chem. Sci.* **8**, 1954–1959 (2017).
46. Cartwright, K. C. & Tunge, J. A. Decarboxylative elimination of n-acyl amino acids via photoredox/cobalt dual catalysis. *ACS Catal.* **8**, 11801–11806 (2018).
47. Hu, X., Zhang, G., Bu, F. & Lei, A. Selective oxidative [4+2] imine/alkene annulation with H₂ liberation induced by photo-oxidation. *Angew. Chem. Int. Ed.* **57**, 1286–1290 (2018).
48. Kalsi, D., Dutta, S., Barsu, N., Rueping, M. & Sundararaju, B. Room-temperature C–H bond functionalization by merging cobalt and photoredox catalysis. *ACS Catal.* **8**, 8115–8120 (2018).
49. Sun, X., Chen, J. & Ritter, T. Catalytic dehydrogenative decarboxyolefination of carboxylic acids. *Nat. Chem.* **10**, 1229–1233 (2018).
50. Liu, W.-Q. et al. Cobaloxime catalysis: selective synthesis of alkenylphosphine oxides under visible light. *J. Am. Chem. Soc.* **141**, 13941–13947 (2019).
51. Meng, Q.-Y., Schirmer, T. E., Katou, K. & König, B. Controllable isomerization of alkenes by dual visible-light-cobalt catalysis. *Angew. Chem. Int. Ed.* **58**, 5723–5728 (2019).
52. Cao, H. et al. Photoinduced site-selective alkenylation of alkanes and aldehydes with aryl alkenes. *Nat. Commun.* **11**, 1956 (2020).
53. Constantini, T. et al. Aminoalkyl radicals as halogen-atom transfer agents for activation of alkyl and aryl halides. *Science* **367**, 1021–1026 (2020).
54. Takizawa, K. et al. Cobalt-catalyzed allylic alkylation enabled by organophotoredox catalysis. *Angew. Chem. Int. Ed.* **58**, 9199–9203 (2019).
55. Kojima, M. & Matsunaga, S. The merger of photoredox and cobalt catalysis. *Trends Chem.* **2**, 410–426 (2020).
56. Dempsey, J. L., Brunschwig, B. S., Winkler, J. R. & Gray, H. B. Hydrogen evolution catalyzed by cobaloximes. *Acc. Chem. Res.* **42**, 1995–2004 (2009).
57. Artero, V., Chavarot-Kerlidou, M. & Fontecave, M. Splitting water with cobalt. *Angew. Chem. Int. Ed.* **50**, 7238–7266 (2011).
58. Bock, C. R. et al. Estimation of excited-state redox potentials by electron-transfer quenching. Application of electron-transfer theory to excited-state redox processes. *J. Am. Chem. Soc.* **101**, 4815–4824 (1979).
59. Lowry, M. S. et al. Single-layer electroluminescent devices and photoinduced hydrogen production from an ionic iridium(III) complex. *Chem. Mater.* **17**, 5712–5719 (2005).
60. Izawa, Y., Pun, D. & Stahl, S. S. Palladium-catalyzed aerobic dehydrogenation of substituted cyclohexanones to phenols. *Science* **333**, 209–213 (2011).
61. Ito, Y., Hirao, T. & Saegusa, T. Synthesis of α,β -unsaturated carbonyl compounds by palladium(II)-catalyzed dehydrosilylation of silyl enol ethers. *J. Org. Chem.* **43**, 1011–1013 (1978).
62. Yu, J.-Q., Wu, H.-C. & Corey, E. J. Pd(OH)₂/C-mediated selective oxidation of silyl enol ethers by tert-butylhydroperoxide, a useful method for the conversion of ketones to α,β -enones or β -silyloxy- α,β -enones. *Org. Lett.* **7**, 1415–1417 (2005).
63. Du, P., Knowles, K. & Eisenberg, R. A homogeneous system for the photogeneration of hydrogen from water based on a platinum(II) terpyridyl acetylide chromophore and a molecular cobalt catalyst. *J. Am. Chem. Soc.* **130**, 12576–12577 (2008).

Acknowledgements

This work was financially supported by the King Abdullah University of Science and Technology (KAUST), Saudi Arabia, Office of Sponsored Research (URF/1/4025).

Author contributions

L.H. and M.R. conceived and designed the project. L.H. performed and analyzed the experiments. T.J. contributed to the scope and application. C.Z., H.Y., and N.Z. conducted and analyzed the H₂ quantification experiments. L.H. and M.R. co-wrote the manuscript. M.R. directed the whole research.

Competing interests

The authors declare no competing interests.

Additional information

Supplementary information The online version contains supplementary material available at <https://doi.org/10.1038/s41467-022-28441-2>.

Correspondence and requests for materials should be addressed to Long Huang or Magnus Rueping.

Peer review information *Nature Communications* thanks the anonymous reviewer(s) for their contribution to the peer review of this work.

Reprints and permission information is available at <http://www.nature.com/reprints>

Publisher's note Springer Nature remains neutral with regard to jurisdictional claims in published maps and institutional affiliations.



Open Access This article is licensed under a Creative Commons Attribution 4.0 International License, which permits use, sharing, adaptation, distribution and reproduction in any medium or format, as long as you give appropriate credit to the original author(s) and the source, provide a link to the Creative Commons license, and indicate if changes were made. The images or other third party material in this article are included in the article's Creative Commons license, unless indicated otherwise in a credit line to the material. If material is not included in the article's Creative Commons license and your intended use is not permitted by statutory regulation or exceeds the permitted use, you will need to obtain permission directly from the copyright holder. To view a copy of this license, visit <http://creativecommons.org/licenses/by/4.0/>.

© The Author(s) 2022